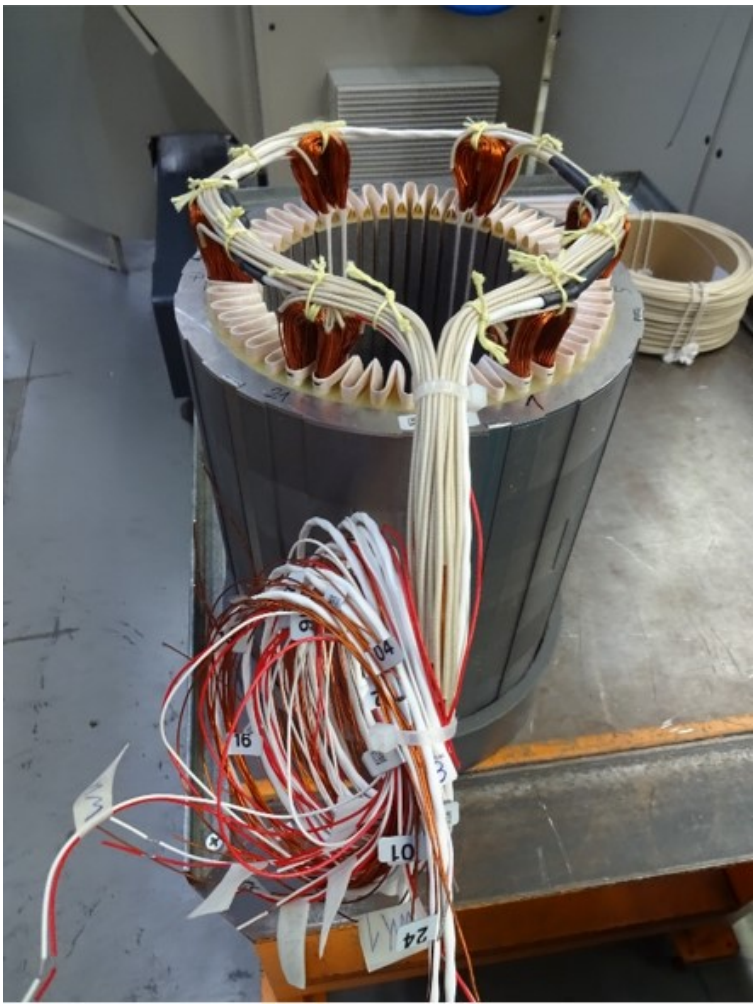

Degradation and Diagnostics of Electrical Machines

RAGHURAM SHANKAR
SMIT DAVE

DEPARTMENT OF ELECTRICAL ENGINEERING

CHALMERS UNIVERSITY OF TECHNOLOGY
Gothenburg, Sweden 2021
www.chalmers.se

Master's thesis 2021

Degradation and Diagnostics of Electrical Machines

RAGHURAM SHANKAR
SMIT DAVE

CHALMERS
UNIVERSITY OF TECHNOLOGY

Department of Electrical Engineering
Division of Electric Power Engineering
Chalmers University of Technology
Gothenburg, Sweden 2021

Degradation and Diagnostics of Electrical Machines
RAGHURAM SHANKAR
SMIT DAVE

Supervisors: Rasmus Andersson and Zhe Huang, Volvo Group Trucks Technology
Examiner: Torbjörn Thiringer, Dept of Electrical engineering

Master's Thesis 2021
Department of Electrical Engineering
Chalmers University of Technology
SE-412 96 Gothenburg
Telephone +46 31 772 1000

Degradation and Diagnostics of Electrical Machines
Raghuram Shankar, Smit Dave
Department of Electrical Engineering
Division of Electric Power Engineering
Chalmers University of Technology
Gothenburg, Sweden 2021

Abstract

Electric Machines are the prime movers in modern electric automobiles. They are subject to different kinds of stresses, often under profiles different to those in traditional applications such as in industries. This causes ageing of the Electric Insulation System (EIS) and is thus a cause of failure. The ageing of the EIS is due to oxidation processes in the insulation and also due to thermal - mechanical stress induced fatigue at high average temperatures. In this thesis work, a test bench has been setup to investigate thermal ageing of the EIS of a test object under thermal cycling. The ageing process has been accelerated by subjecting the test object to currents higher than rated values, thereby producing larger thermal stresses than under regular operating conditions. A Graphical User Interface (GUI) for real time monitoring of test parameters, along with an automated test logic has been developed and tested. The test object has been subjected to 500 cycles of thermal stress from 150°C to 200°C and various parameters have been measured and logged. The impact of the cooling system was also investigated. The results have been plotted and the trends in insulation parameters such as Insulation Resistance (IR), Polarization Index (PI), Dielectric Absorption Ratio (DAR), Insulation Capacitance (IC) and Dissipation factor (DF) are used to describe the State of Health (SOH) of the EIS.

Keywords: Electric Machine, Electric Vehicle, Electric Insulation System, Condition Monitoring, Thermal degradation, Thermal Cycling

Acknowledgements

We take this opportunity to thank all those who have helped us in the execution of this thesis work. Foremost we thank our supervisors Rasmus Andersson & Zhe Huang from Volvo Group Trucks Technology for their support, encouragement and trust in us. Furthermore we would like to thank our thesis examiner Prof. Torbjörn Thiringer for his continuous guidance, support and fruitful discussions over the test bench assembly. We would like to thank Tommy Schoug at Volvo Group for his input regarding the data acquisition setup. This work has been carried out at the Department of Energy and Environment at Chalmers University of Technology. We also would like to extend our thanks to Stefan Lundberg, Daniel Pehrman, Artem Rodinov, Nimananda Sharma & Douglas Jutsell Nilsson for their support related to laboratory space and equipment handling.

Raghuram Shankar and Smit Dave
Göteborg, Sweden
June, 2021

Contents

1
Introduction

1.1 Background

The automotive industry is currently undergoing a transition from conventional combustion power to electric and hybrid electric powertrains. This offers numerous advantages such as less moving parts, better powertrain efficiency and of course, lower emissions. Now, the electric machines that drive these automobiles are being used under various driving cycles, which makes their ageing characteristics different from that in traditional applications in industries. It is therefore important to predict the lifetime of these machines to prevent under or over-dimensioning. Hence, a more targeted approach with regard to performance and lifetime of these traction electric machines is required.

1.2 Previous Work

A comprehensive survey of electric machines currently in use for automotive traction applications is presented in [1] and [2]. It can be seen that the Permanent Magnet Synchronous Machine (PMSM) is the most popular electric machine for automotive applications. [3] lays out the concept of tracking changes in insulation parameters with weibull distributions of breakdown voltages to quantify insulation ageing in electric machines. In [4], methods and models used for lifetime studies have been reviewed. [5] describes an approach of using Mean Time Between Failures to predict the lifetime of electric machine insulation. In [6], various industry standards and safety practices are provided for electrical insulation testing using Megger instruments.

1.3 Aim

This thesis work aims to design and build a test rig setup to be used for durability tests with a cycling temperature. The main functionality of the test is to include power cycle testing through control of DC current, control of the cooling circuit and real time monitoring of test rig parameters. A control logic is to be developed to run the power cycle tests and to shutdown the test if the parameters are not within the safe operating regions.

1.4 Scope

This thesis work deals with hardware assembly of the test rig setup. Along with this a data acquisition system was developed to read and log test rig parameters for monitoring and offline analysis. As we aim to study the degradation of the Electrical Insulation System (EIS) a series of tests will be performed on the test object to measure the insulation parameters. These insulation parameters include the Insulation Resistance (IR), Insulation Capacitance (IC) and Dissipation Factor (DF) and Coil Inductance.

2
Theory

2.1 PMSM

Different topologies of electric machines for application in electric vehicles have been studied in [2]. The most popular types of machines are Induction Machines (IM) and Permanent Magnet Synchronous Machines (PMSM) [7]. A PMSM has high power density, high starting torque and high efficiency, but is expensive and requires complex control algorithms for operation under field weakening. These machines in Electric Vehicle applications are usually power by a large battery pack through three-phase power electronic inverters. A PMSM typically consists of a stationary rotor, with insulation & magnets and a rotating rotor.

2.2 Stator Winding

There are three main components in the stator, namely the stator core, copper conductors and the insulation. In a motor application, the current in the stator produces a rotating magnetic field which in turn forces the rotor to move. The major component of the stator is the electrical insulation. It is a passive component and does not contribute to the generation of the magnetic field. The role of the insulation is to prevent short circuits between two windings or between windings and ground. Hence it is an integral component of the motor. The insulation system also plays the secondary role of being a thermal conductor in indirectly cooled machines and also serves as a housing to the windings and prevents free motion of the conductors in the stator slots. The life and age of an electrical machine is determined by the insulation system rather than the copper windings itself [8]. Some properties of electrical insulators, including resistivity, dielectric strength and their applications are given in [9] and [10].
There are three types of stator winding structures

- Random Wound
- Form Wound using multi turn coils
- Form wound using Roebel Bars

2.3 Electrical Insulation System (EIS)

The electrical insulation system in a stator of an electric machine contains several different components and functions. The main function of the EIS is to prevent

electrical shorts, provide proper heat transfer path from the conductors to the cooling jacket / heat sink and to prevent the conductors from vibrating in the presence of the magnetic forces [11]. The EIS is divided into the following system components:

- Strand insulation
- Turn Insulation
- Groundwall (or ground or earth) insulation

In addition to the following system components the EIS also contains high voltage stress relief coatings and end winding support.

2.3.1 Strand Insulation

The function of strand insulation is to provide insulation in slot turns. Also designers add extra reinforcements to boost the insulation strength in areas of high stresses. To meet current requirements, the cross section of the strands are greater which causes mechanical problems such as bending and maintaining form while stator winding. Hence designers choose to reduce the copper conductor cross section. This can also be beneficial in terms of electrical aspects. The skin effect is reduced due to its smaller cross section and losses due to eddy currents in conductors of greater cross section can also be prevented. The strand insulation is applied on the copper conductor which carries the motor current, it produces I^2R losses. The losses generate heat and expose the strand to maximum thermal stress. Hence it is necessary for the strand insulation to have good thermal properties[8].

2.3.2 Turn Insulation

The turn insulation is present to prevent shorts between the winding turns. If a short occurs in between two turns of a winding/coil the current flowing through the coil will follow transformer law

$$n_p I_p = n_s I_s \tag{2.1}$$

where n is the number of turns in primary or secondary, and I represents the current flowing in the primary or secondary. The short introduces circulating current giving rise to thermal hot spots in slot and coil. This turn to turn fault is usually followed by a ground fault due to the melted copper as a result of overheating through the ground wall insulation. This calls for an effective turn insulation design for longer stator lifespans[12].

2.3.3 Ground Wall Insulation

The ground Wall insulation separates the copper strands from the grounded core of the stator. Failure of ground wall insulation causes a ground fault making the motor go out of operation. These faults are detected by the Insulation monitoring devices of the vehicle and lead to the tripping of the main tractive system relay. Hence, this is critical for safe operating of the motor and vehicle. For a longer service span the ground wall must meet the requirements of the TEAM(Thermal, Electrical, Ambient and Mechanical) stresses.

2.3.4 Mechanical Support in the Slot

The windings are subjected to large forces during the motoring operation. The forces experienced are at two times the frequency of the AC voltage supplied by the power electronic inverter controlling the motor. If a phase to phase fault occurs the fault current is I^2 as per the equation

$$F = \frac{kI^2}{d} kN/m \tag{2.2}$$

where I is the rms current, d is the width of the stator slot in meters and k is 0.96 and F is the force acting onto the coil. Hence, the coils must be restrained from moving. If not, then the coils become loose and will cause abrasion of the insulation or may lead to fatigue cracking of the insulation which eventually will lead to a short. This is undesirable for a longer lifespan. This is avoided by introducing a non magnetic and non conductive wedge as a mechanical support which serves as a part of the EIS.

2.3.5 Mechanical Support in the End-Winding

The end winding is present to allow safe electrical connections between coils in series and to connect to other parallels. Machines with higher voltage rating will have a higher creepage distance between the stator core and the connections. The end windings require support to avoid movement. Without support the coils become loose and will cause abrasion of the insulation or may lead to fatigue cracking of the insulation which will eventually lead to a short similar to a slot shorting. Usually the epoxy used in VPI is sufficient for this purpose or a specialized support ring or bracing ring is introduced during VPI for additional reinforcement.

2.4 Degradation in Electrical Machines

There are many stresses that cause insulation degradation in the stator. They are broadly classified as TEAM (Thermal, Electrical, Ambient and Mechanical) stresses. It is important to note that stresses maybe present throughout the lifespan of the electrical machine or only for a brief period. Generally if a failure is caused by a constant stress it implies that the failure is directly proportional to the number of operating hours. Whereas the failure caused by transient stresses is proportional to the number of transients experienced by the electrical machine.

2.4.1 Thermal Stress

Thermal stress is the most acknowledged cause of insulation degradation and is also the reason for an ultimate failure of the EIS. The EIS must be tested for its thermal capabilities intensively before implementing it into the electrical machine design. Insulation installed in modern day machines undergo an oxidation process which causes delamination of windings, brittleness of insulation and material deterioration.

The oxidation rate of reaction is defined by the Arrhenius rate law given by the equation

$$L = Ae^{B/T} \tag{2.3}$$

where L is life of insulation in hours, T is temperature in Kelvin and A & B are assumed to be constants. It can be noted from the equation that every 10°C rise in temperature reduces the life of the winding by 50%. The limitations of (2.3) are that it is only valid for relatively high temperatures and modelling of more than one chemical process is not entirely possible in a first order system.

2.4.2 Electrical Stress

Power frequency electric stress has high impact on ageing for machines rated below 1000V. Power frequency voltage can only contribute to ageing if there is a presence of partial discharges. Partial discharges (PD) are small electric sparks which are present in the air cavity / insulation surface due to the build of charges due to excitation current and potential differences. The electric stress level (E in kV/mm) due to the presence of PD can be represented by the inverse power model given by the relation

$$L = cE^{-n} \tag{2.4}$$

where L is life of insulation in hours, c is constant and n is the power law constant. The power law constant varies between 9 to 12 for electrical machine insulation systems. If we consider n to be 10, then a stress of twice the magnitude will reduce the life of the insulation by 1000 times. This proves that the electric stress has a significant impact on the age of the machine if PD occur.

2.4.3 Ambient Stress

Ambient stress is defined as a collection of factors which occur in the surroundings of the electrical machine. The factors can be of the following nature:

- Presence of moisture in the windings
- Humidity in the surrounding
- Oil leakage from bearings of the transmission or gearbox
- Chemical exposure due to site operations
- Abrasive particles in the coolant
- Brake shoe/pad wear and tear particles
- Debris and dirt
- Radiation exposure

Each of the above factors affect the insulation of the machine individually and they also have combined impacts on the insulation health.

2.4.4 Mechanical Stress

Mechanical stress originate from three different sources.

- High centrifugal forces originating from the rotor which distorts and tends to crush the insulation

- The power frequency current which gives rise to high electromagnetic forces which in turn generate vibrations in stator and rotor slots.
- External vibrations experienced due to the loading of the motor which are experienced onto the motor shaft first and are transferred outwards to the rest of the machine.

There are no models or equations which exist to physically model these phenomena and hence it needs to be studied practically on system levels using various measurement equipment.

2.5 Accelerated Ageing Test

Accelerated testing is performed to speed up the ageing of the test specimen by increasing stress levels. Accelerated ageing provides ground for faster development of insulation systems as one cannot wait for 15 - 20 years for a component to fail and then re-design the part.

2.5.1 Thermal Endurance Tests

Thermal stress is the widely used as degradation cause when only one type of insulating material is in evaluation. Every organic material has an activation energy requirement. Imposing thermal stress onto the material increases molecular energy and aids the reaction rate. However only thermal ageing is not sufficient in order to study the EIS. Other components of an electrical machine made of inorganic and metallic material also need to be accounted for. This calls for thermal identification of insulation systems as well as electrical components [13].

Table 2.1: Thermal Classification of Machine Insulation Material (from IEC 60085)

Numerical Classification	Letter Classification	Temperature°C
105	A	105
130	B	130
155	F	155
180	H	180

2.5.2 Test Standards

A number of test standards were followed and studied during the entire duration of the thesis work and a test rig was designed keeping in mind the following IEC standards

Table 2.2: Reviewed standards related to thermal cycle degradation of insulation material, enameled wires and insulation systems of electrical machines

Standard No.	Type of specimen	Description
IEC 60085 [14]	Insulation material	Thermal classification of electrical insulation material/materials
IEC 60216 [15]	Insulation material	Thermal classification of electrical insulation material/materials
IEC 61857 [16]	EIS of random wound windings	Electrical insulation systems thermal evaluation
IEC 60611 [17]	Thermal Endurance of EIS	Guide for the Preparation of Test Procedures for Evaluating the Thermal Endurance of Electrical Insulation Systems

2.6 Theoretical - Resistance per coil

There are 110 strands per slot as we have 55 turns per coil. Table 2.3 shows the winding parameters.

Table 2.3: Winding Parameters

Parameter	**Value**
Strand Diameter	0.85 mm^2
Conductivity of copper	1.68 x $10^-8 \Omega m$
Cross Section Area of single strand	0.567 x $10^-6 m^2$
Active Length of single strand	240 mm
Length of strand for 1 turn	500 mm
Total Length for 1 strand	11 m

where,

$$R_{strand} = \frac{\rho \times l}{A} = \frac{1.68 \times 10^-8 \times 11}{0.567 \times 10^-6} = 0.3\Omega \tag{2.5}$$

$$R_{coil} = 0.5 \times 0.3\Omega = 0.15\Omega \tag{2.6}$$

3

Case Set-up

This chapter explains the methodology adopted to build up the test rig according to relevant tests, describes the various test setups for different measurement techniques and the control strategies implemented on the bench.

3.1 Test Rig Design

The first step taken in the test rig design was to start with a connection diagram for the electrical circuitry, cooling circuit and the wiring connections for the sensors present in the rig and the ones that are potted inside the motorette. Figure 3.1 shows the overall layout of the test bench.

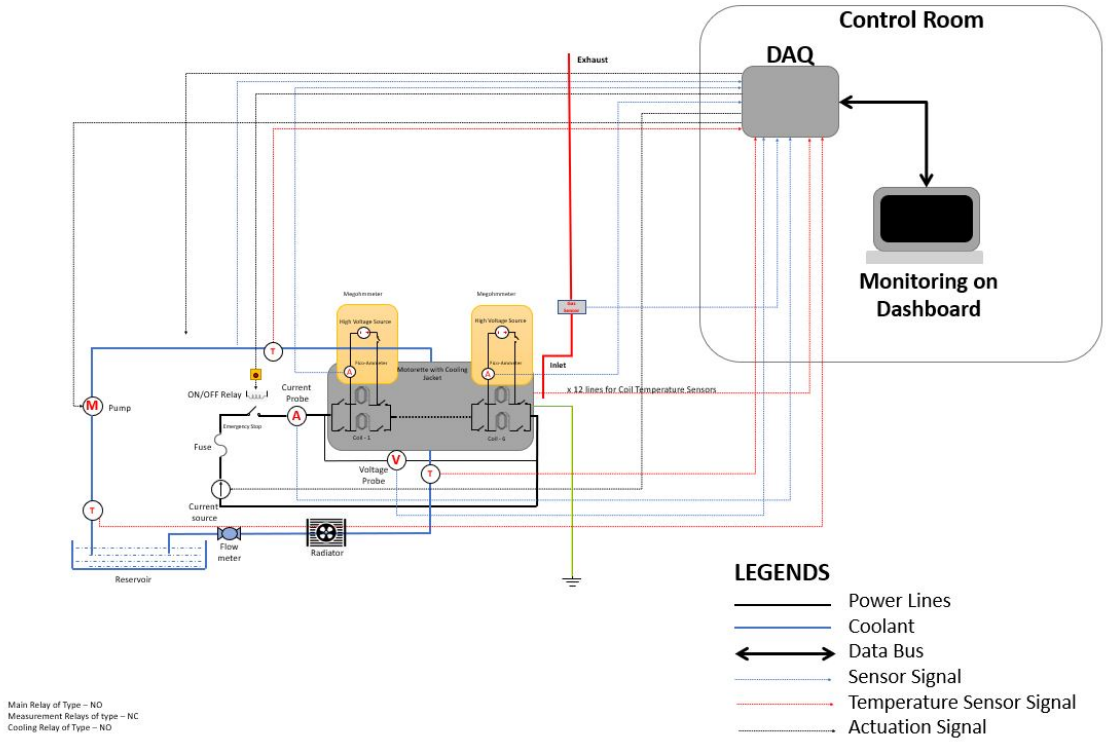

Figure 3.1: Connection Diagram

3.1.1 Temperature Sensors

The temperature sensors used in the motorette specimen are of the platinum RTD type which are 2 wire PT100s. There are 12 PT100s potted into the motorette and 3 more will used in the test bench to monitor the temperature of the coolant at inlet point of the radiator, at the outlet of the radiator and to measure the hot air exhaust temperature at the radiator. The PT100 temperature sensors are available in a 2 wire, 3 wire and 4 wire construction. Table 3.1 shows a comparison between all three types of construction.

Table 3.1: Comparison between all three construction types of PT100

Construction	2 Wire	3 Wire	4 Wire
Advantages	Simple RTD Connection	Voltage drop across the line resistance are compensated.	Voltage drop across the line resistance are compensated.
	Only one current source is required.	Allows complete utilization of the input range, no offset caused by the RTD itself.	Allows complete utilization of the input range, no offset caused by the RTD itself.
Disadvantage	Voltage drop across the line resistance.	Needs two current sources.	Needs two current sources and Four connections are used for every sensor.

The PT100 is a platinum RTD, which has a resistance of 100 Ω at 0 °C. The Callendar-Van Dusen equation describes the relation between resistance and temperature of a platinum RTD. The resistance can be found as

$$R_T = R_0(1 + aT + bT^2 + c(T - 100)T^3) \tag{3.1}$$

where R_T is the resistance at temperature T °C, R_0 is the resistance at 0°C , a, b and c are the temperature coefficients of the given RTD. The PT100 has the following parameters:

Table 3.2: PT100 parameters

Parameter	Value
R_0	100
a	0.039083
b	-5.77e-7
c	-4.183e-12

The temperature sensors are placed inside the motorette and figure 3.2 shows the positioning of the primary and the reserve temperature sensor.

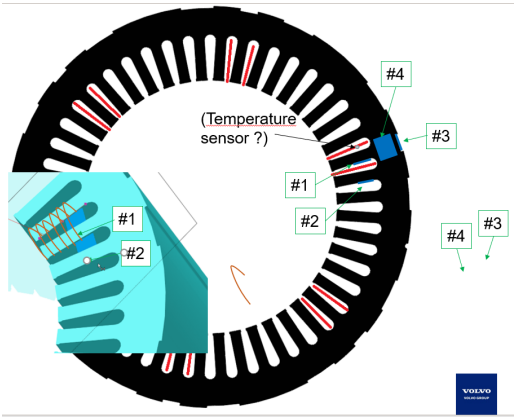

Figure 3.2: Position of temperature sensors inside the motorette

3.2 Current Measurement

The current probe used in the test bench is a Tektronix P6303 with an AM503 current probe amplifier. The amplifier is used to set the current/div, bandwidth, DC bias level and also degauss the current probe. The output of the current probe is of the female BNC type which can be connected to any 50Ω termination such as an oscilloscope or data acquisition system.

The current probe is connected as can be seen in the figure 3.1. This probe is capable of measuring up to 100A DC current and hence is ideal for our application.

The DC current for accelerated ageing test is calculated to be 30A and the rated coil current is 15A. The calculation will be presented in the motorette testing section of this chapter. The output voltage from the current probe amplifier is in the range of ± 80 mV. The measurement from the probe is first calibrated using the measurement module with a DC offset at zero current. Then, the change in voltage is noted per ampere of current. It was also noted that the values of DC bias and voltage/current ratio is different at different settings of the current probe amplifier. Thus, the calibration process is to be repeated for different settings and every time the setup is to be run. The DC bias can be used as a correction factor in CSM config, while the voltage/current ratio is to be updated in the Python data acquisition script.

The current in the main HV circuit is measured using a current probe and amplifier setup as our DAQ system cannot measure current directly. This means that the output from the current amplifier, which is a voltage proportional to the current flowing in the circuit needs to be postprocessed into a current value.
Thus, the current offset value and voltage measured per ampere of current flowing in the circuit was found. These values are known to change and needs to be calibrated from time to time.

Equation (3.2) shows the offset & voltage per ampere values and the equation used

to calculate the current flowing in the main circuit. Figure. 3.3 shows the test setup with the current probe measuring current in the main HV circuit.

$$Offset = 1.138e^{-1} \tag{3.2}$$

$$Volt_{perA} = 2.670e^{-1} \tag{3.3}$$

$$Current(A) = \frac{Volt_{measured}(V) - Offset(V)}{Volt_{perA}(V/A)} \tag{3.4}$$

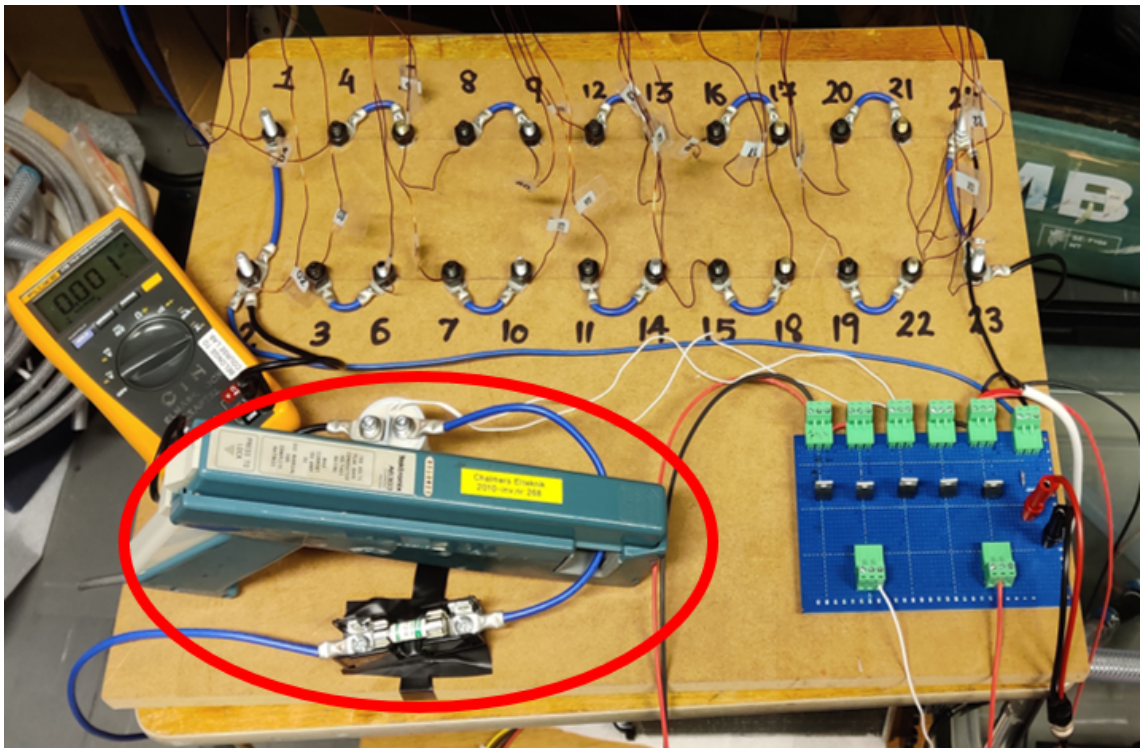

Figure 3.3: Current measurement

3.3 Voltage Measurement

The AD Scan MM can measure voltages upto 60VDC. However, we found that the voltage across the test coils ranges from 80V to 140V at 20A current up to 200 °C. Thus, we used a resistor based voltage divider to step down the voltage for measurement using the CSM module. By knowing the resistor values, we can calculate the actual current across the main HV circuit.

$$V_{out}(V) = \frac{10K}{10K + 58K} \cdot V_{in} = 0.1471 \cdot V_{in}(V) \tag{3.5}$$

$$V_{in}(V) = \frac{1}{0.1471} \cdot V_{out} = 6.8 \cdot V_{out}(V) \tag{3.6}$$

Figure 3.4 depicts the voltage divider setup used and Figure 3.5 shows the connection of the voltage measurement with the main circuit.

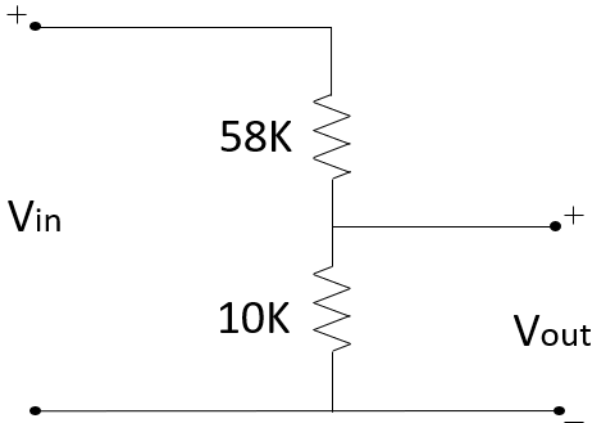

Figure 3.4: Voltage divider for stepping down voltage

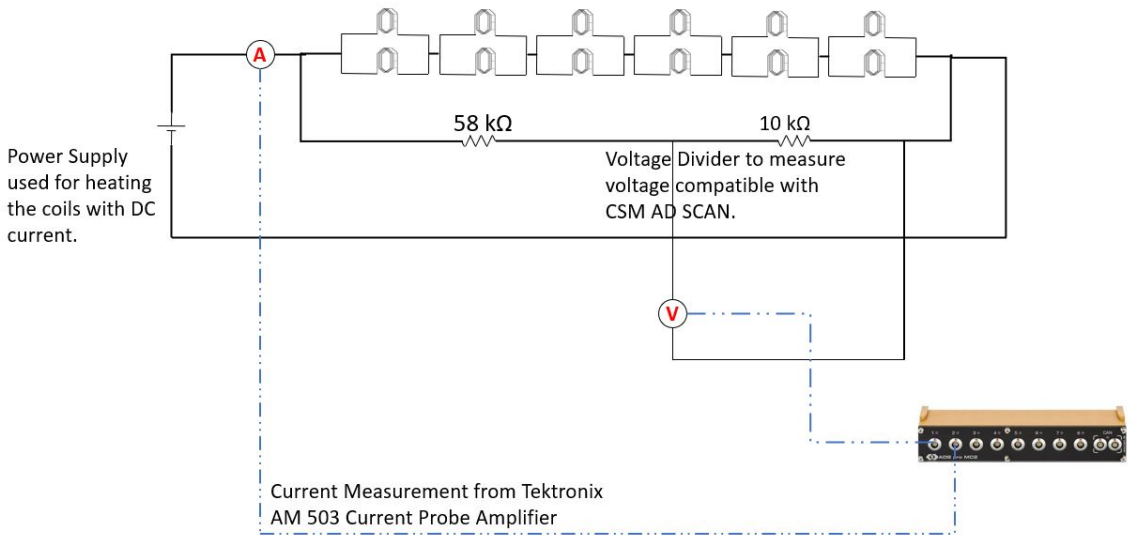

Figure 3.5: Voltage measurement

3.4 Winding Connections

The motorette comprises of 6 coils and each coil has 2 strands in parallel. There are a total of 55 turns per strand which makes 110 turns per coil. All the coils are connected in series so that a current of same magnitude flows through the coils and then a comparison between insulation degradation can be done between the 6 coils. The connection is shown in figure 3.6

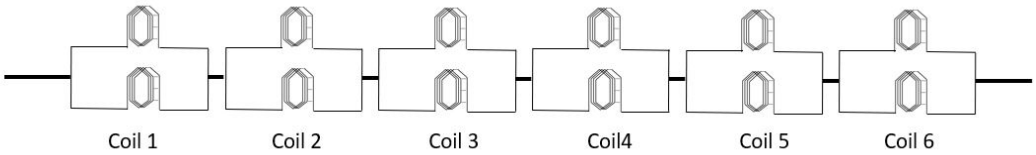

Figure 3.6: Series connection of coils

3.5 Electrical Circuit Calculations

This section shows all the calculations required to dimension all the components on the bench and validates the choice of components selected for the bench.

3.5.1 Measurement of Resistance per strand

A practical method was used to measure the strand resistance using the V/I method. This was done for both the strands in a single coil and a similar results were obtained for all the coils. Figure 3.7 shows the measurement arrangement and Table 3.3 shows the measurements.

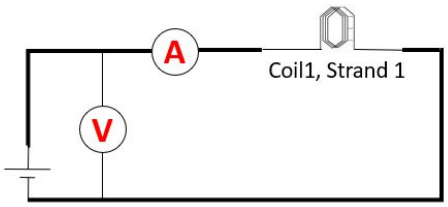

Figure 3.7: Measurement Arrangement

Table 3.3: Strand Resistance Measurements for Coil 1

Strand No.	**Voltage(V)**	**Current(A)**	**Resistance(Ω)**
Strand 1	4.508	3.171	1.4216
Strand 2	4.510	3.176	1.4335

From the readings we observe that the coil resistance is 0.713 Ω. This value is 4.75 times higher than the theoretical calculations and we need to dimension our test bench components and decide the test bench parameters on basis of this.

3.5.2 Current Calculation for Accelerated Ageing

The table 3.4 below shows the parameters of the complete electric machine designed for Volvo Group Trucks Technology.

Table 3.4: Electric Machine parameters

Parameter	Value
Peak Current	300A
No of Slots	48
Pole Pairs	4
Coils in parallel per phase	8
Strand per coil	2
Turns per strand	55

$$Current_{coil} = \frac{300}{8} = 37.5A_{coil} \tag{3.7}$$

The actual machine comprises of 22 turns per slot. Hence this current is multiplied by the number of turns in the actual machine.

$$Current_{slot} = 37.5 \times 22 = 825A_{slot} \tag{3.8}$$

$$Current_{parallelpath} = \frac{825}{2} = 412.5A_{parallelstrand} \tag{3.9}$$

$$Current_{strand} = \frac{412.5}{55} = 7.5A_{strand} \tag{3.10}$$

$$Current_{acceleratedageing} = Current_{strand} \times 2 = 15.0A \times 2 = 30.0A \tag{3.11}$$

The accelerated ageing test is done keeping in mind double the peak current i.e. 600A.

3.5.3 Voltage Calculation

The voltage required to produce a constant current of 32.727A for a series resistance of 4.2 Ω is

$$Voltage = Current_{acceleratedageing} \times R_{series} = 32.727A \times 4.2\Omega = 137.45V \tag{3.12}$$

This is done by operating two of the SM300-20 Delta Elektronik Power supply units in parallel. So that we have an operating range of 300V and 40A for the test bench.

3.5.4 Operating Voltage and Current

Due to the limitation on availability of equipment the operating voltage and current on the test bench was set to 150V and 20.4A and the thermal cycles are run in a continuous current mode of the power supply.

3.6 Dimensions of Cooling Circuit

The cooling circuit comprises of a Bilge Pump with a maximum flow rate of 32l/min, a radiator assembly and the cooling jacket of the motorette. These components are connected pipes of inner diameter of 18 mm and an outer diameter of 25 mm. The attachment points are sealed with steel hose clamps and tightened to avoid any air and water leakage from the system.

It is very much necessary to not have any air bubbles in the system for maximum cooling efficiency. This is taken care of by bleeding all the components in the cooling circuit before making any connections between them.

Table 3.5: Specification of Radiator

Parameters	**Value**
Fan Dimensions	119x119x25
Fan Max RPM	3000
No. of Fans	2
Air Flow rate	83x2 CFM (cubic feet per minute)
Core Dimensions	245x157x40

3.7 Data Acquisition Setup

In our test rig setup, data acquisition is done using modules from Computer-Systeme-Messtechnik (CSM) GmbH. We have used 5 modules in total, with the sensor setup and channels as given in Table 3.6.

Table 3.6: CSM Modules used for Data Acquisition

Module	PT Scan MM	AD Scan MM	Out MM
Number of modules	3	1	1
Channels per module	4	8	8
Function	Measure temperature using RTD	Measure analog voltage	Output voltage, current and digital signals
Connector to sensor	LEMO 0B, 6-pole, Code A	LEMO 0B, 6-pole, Code A	LEMO 1B, 2-pole, Code A

These modules communicate with each other and the main host computer using a CAN bus. Thus, each module is daisy chained, where a computer is connected to the CAN bus through our CAN bus interface, the Kvaser Memorator Professional HS/HS. The other end of the CAN bus has a CAN bus terminator, which is a 120Ω resistor. The CAN bus runs through each modules using the CAN bus cables which

connect through LEMO 0B, 5-pole, Code G connectors.

The CAN bus and all of the modules present are configured using the CSM Config software. After configuration of each channel on each module, we obtained two CAN database (dbc) files. These are text files which contains information for decoding raw CAN data to human readable form. They are also used for encoding messages to be sent on the CAN bus. One of the dbc files contained information for handling inputs from the bus, while the other contained information for handling outputs to the bus.

Then, a Python script was written to read the dbc files, establish a connection to the bus through the CAN bus interface and send & receive messages. We used open source libraries and APIs to achieve this.

A custom GUI application, written using the Tkinter library in Python was developed as a dashboard for the test rig setup. The application allows us to monitor sensor values in real time, control the relays & cooling circuit and also monitor the CAN bus.

3.8 Graphical User Interface

A Graphical User Interface (GUI) is a type of User Interface (UI) that allows us to interact with electronic devices using icons and indicators instead of text based interfaces. It can be very helpful in visualizing performance and diagnostics of any setup.

A custom GUI has been developed from scratch, designed to work specifically for this bench setup.

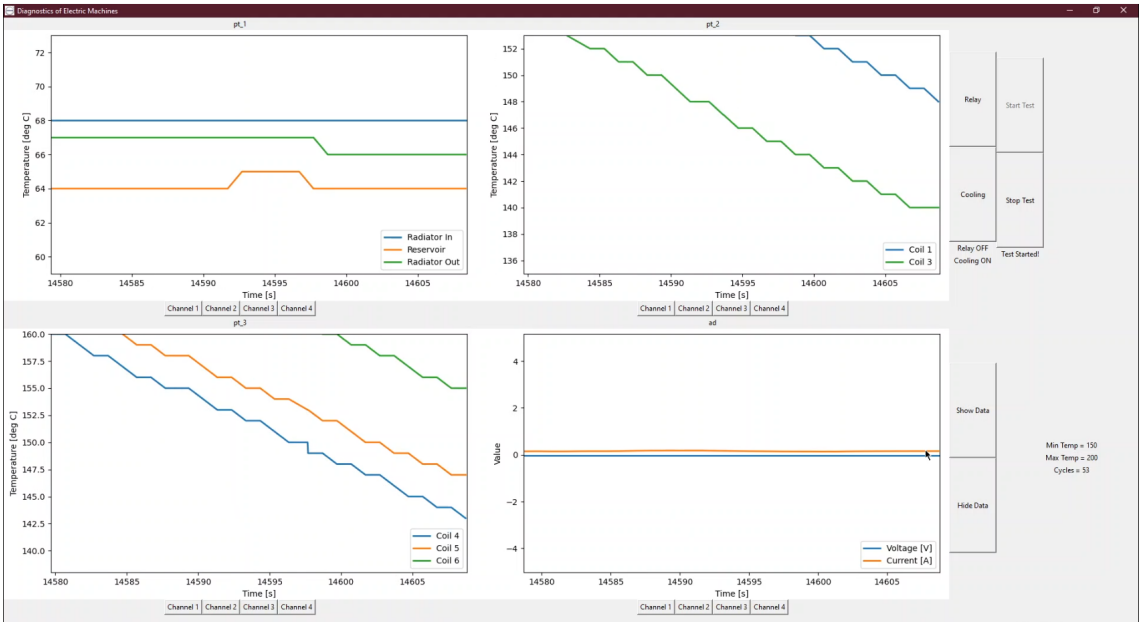

Figure 3.8: Graphical User Interface

Figure 3.8 shows the developed GUI for the test bench setup. In the configuration that was chosen for testing, there were 4 plots with 4 channels each as we used 4 CSM Minimodules. This includes three PT Scan MiniModules for measuring temperature of the test object & cooling system and one AD Scan MiniModule for measuring current & voltage in the main HV circuit. The functionalities of the GUI are discussed in the following sections.

3.8.1 Display plots of temperatures, current and voltage

We are interested in measuring and logging the temperatures inside the test object, the voltage across the coils and the current flowing through the test object. When the test is running, we are required to monitor the said parameters in real time. The data acquisition, the GUI and the data logging are setup to work at a sampling rate of 1 Hz. This means that data is received from the CSM modules, plotted on the GUI and logged in a spreadsheet once every second. This sample rate was chosen as it was adequate for using the data logged for further analysis while not being too computationally expensive for the GUI for updating in real time. Channel selectors are also available for the user to toggle channels to be displayed in each plot. Each channel is also color coded and the legend shows the color of each channel.

3.8.2 Manual control of main relay and cooling

Two buttons are available for control of main relay and cooling circuit. Clicking on them toggles them ON and OFF. Also, labels are displayed below these buttons to indicate their current status.

3.8.3 Input parameters for automated testing

The user can also input the desired minimum temperature, maximum temperature and number of cycles for the automated test. The input is also checked for validity and the test is stopped in case of invalid input.

3.8.4 Start and stop automated test functionality

The user can start and stop the automated test with the desired input parameters at any point of time using two buttons Labels display the current status of the test automation, the minimum and maximum temperature given by the user and the number of cycles currently completed.

3.8.5 Show and hide test data

The user can also plot data from an ongoing test by using these two buttons. When the show data button is clicked, new plots outside the root window of the GUI pop up to display the temperatures, currents and other measurements of the ongoing test for analysis on-the-go.

3.8.6 Data Logging

Data received from the CAN bus every second is plotted in the GUI and logged in a CSV file. These CSV files are generated every time the root window is closed. The relative time, system time and data from all of the channels on each CAN module is logged. When a test cycle is completed, a temporary log file is created for redundancy in case of any mishaps during the automated test.

3.8.7 Test Environment

A test environment, which can be run without a CAN bus was also setup. Here, data is read from a CSV containing mock-up data and plotted in the GUI. This allows us to create an environment to test all of the functionality of the GUI without requiring a CAN bus to be connected. It was used extensively to test all of the functionalities and ensure they would work before porting them to the live bench GUI.

3.9 CSM Modules

A total of four CSM modules were used for data acquisition and control of our test bench setup.

Table 3.7: Overview of CSM modules used

Module	**Functionality**	**Total channels used**	**Quantity**
PT Scan MM	Measure temperature	9	3
AD Scan MM	Measure current & voltage	2	1
AD Out MM	Control of relay and cooling	2	1

An overview of the setup is shown in Table 3.7.
The pt_1 measures temperatures in the cooling circuit and the pt_2 and pt_3 modules measure coil temperatures. The *ad* module measures current and voltage across the main circuit, while the *out* module is used for control of the main relay and cooling circuit.

Table 3.8: Configuration of CSM modules used

Channel	**pt_1**	**pt_2**	**pt_3**	**ad**	**out**
1	Radiator in	Coil 1	Coil 4	Voltage	Main relay
2	Reservoir	Coil 2	Coil 5	Current	Cooling
3	Radiator out	Coil 3	Coil 6	_	_

Table 3.8 shows the configuration of each module for the parameters of interest.

3.10 Driver Circuit and Control

A MOSFET based driver circuit was designed and manufactured to allow hardware compatibility between the CSM modules and the Main Relay, Coolant Pump and Radiator fans. This solution was developed so as to overcome the limitation of the CSM modules which can only provide an excitation current of 20mA. The current requirements from the Relay, Pump and Radiator fan are 450mA, 2.2A and 0.8A respectively.

The MOSFET chosen for this application is IRF3205PBF as it has a low on state resistance of 8 mΩ. The control signals from the OUTMM CSM module are applied to the base of the MOSFET and it is operated as a switch. The connection diagram for the same is presented in figure 3.9

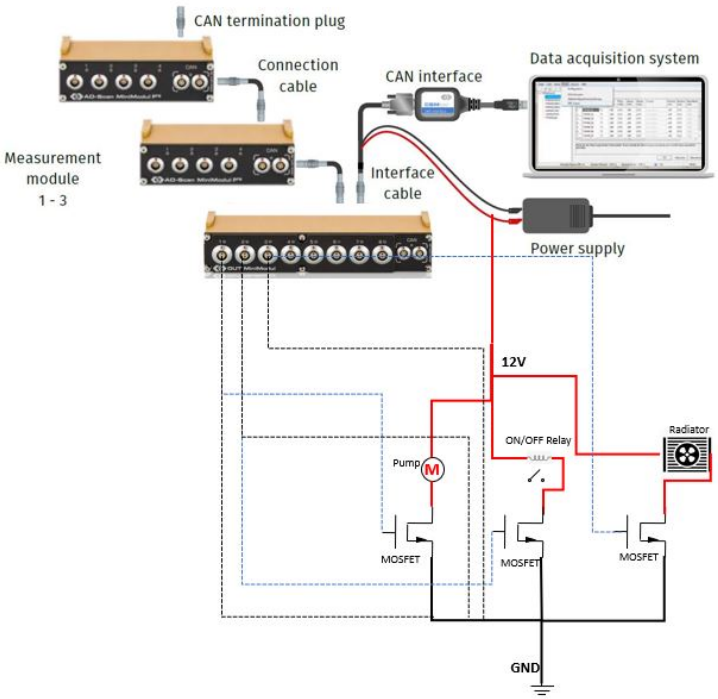

Figure 3.9: Driver Circuit

There are 3 components that are being controlled by this driver circuit and two additional MOSFETs have been added if there is a future need to include more components into the bench such as a 3 way valve, flow meter or a gas sensor for additional monitoring and control over the test bench. The final soldered and assembled driver circuit is as shown in fig 3.10

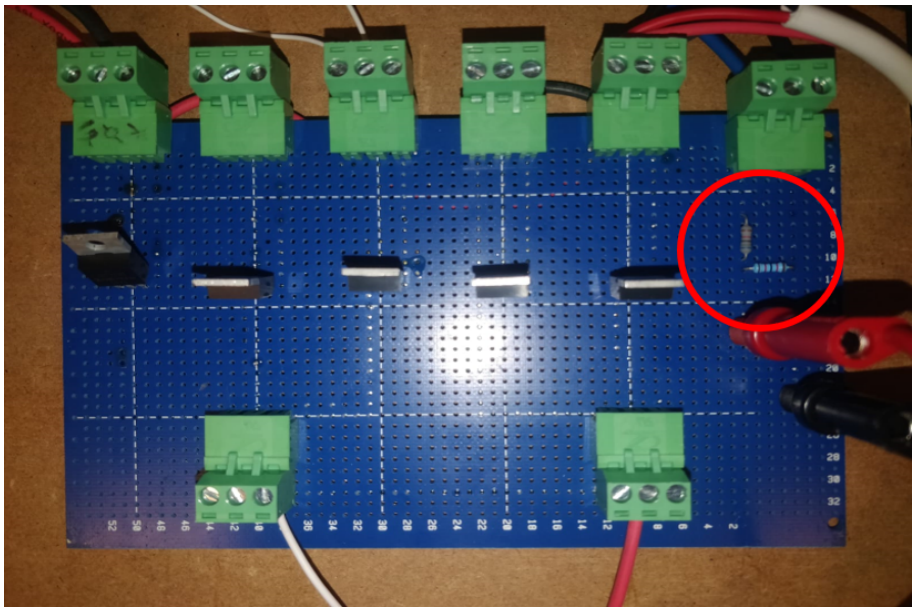

Figure 3.10: Soldered and Assembled Driver Circuit

3.11 Overview of Code

A Python script has been written to perform all the functionalities required for the test bench setup. This includes setting up the CAN bus in the CSM DAQ system, receiving data from the CAN bus, plotting received data in the GUI and logging data in a CSV file. An object oriented approach has been taken to ensure scope for expansion in the future, for easy inclusion or removal of CSM modules. Thus, each part of the GUI is an object of a different class, written to perform a specific task. Member functions in each class are called for performing tasks. The GUI is written using the Tkinter library in Python, which is used specifically to develop custom GUI applications. The Matplotlib, Numpy and Pandas libraries are used for data processing and plotting. The Python-can and Cantools libraries are used for communication with the CAN bus.

3.12 Test Bench Logic

The logic flow diagram for the test bench logic for the automated test is shown in Figure. 3.11. Before the test starts, the user is asked to input the minimum temperature, maximum temperature and the total number of cycles to be run. The objective of the automated test is to first heat the test object from ambient temperature (T_{amb}) to the maximum temperature (T_{max}), then cool it down to the minimum temperature (T_{min}), then heat it back up to T_{max}, and so on until the desired number of cycles is completed. This is defined as thermal cycling and is a used to accelerate thermal ageing in the test object.

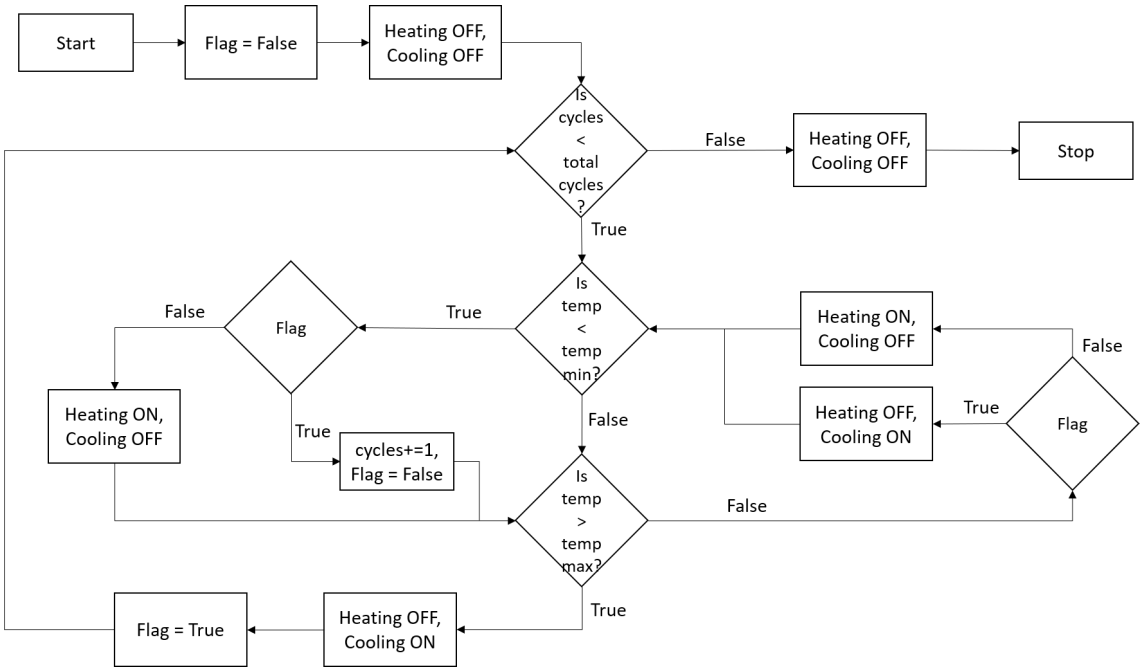

Figure 3.11: Bench automated test logic

At all times, the maximum temperature of all the coils is defined as the temperature of the test object ($T_{machine}$). Also, the main relay and cooling system are never switched ON at the same time. This is to ensure that heating and cooling the test object is achieved at the quickest possible time at the selected current.

A cycle is defined to be completed when the $T_{machine}$ reaches T_{min} when it is being cooled. A counter variable keeps track of the number of cycles completed and the test stops when the number of cycles reaches the user input value.

In the code, a boolean variable Flag is used to determine whether the test object is currently being heated (False) or cooled (True). Initially, Flag is set to False to heat up the test object to T_{max}. There are 3 different scenarios in the automated test:

Case 1: $T_{machine}$ **is less than** T_{min} In this scenario, the heating is turned ON and cooling is turned OFF. The Flag variable is set to False to heat the test object. Also, if Flag was previously set to True, which means that the test object was being cooled to T_{min}, then the number of cycles completed is incremented, and a temporary log file is created.

Case 2: $T_{machine}$ **is greater than** T_{min} **and** T_{max} If Flag was previously set to True, then we want to continue cooling. If Flag was set to False, then we we want to continue heating.

Case 3: $T_{machine}$ **is greater than** T_{max} We set the Flag to True, and start cooling the test object.

3.13 Motorette Testing

A test setup is created to study the degradation in EIS under dynamic thermal stresses and to study the degradation characteristics in order to improve the monitoring modes in the vehicle. The accelerated ageing tests are also carried out on this segmented stator also called as the Motorette.

The motorette specimen was received from Volvo Group Trucks Technology and it contains only six coils with two strands in parallel per coil. Figure 3.12 shows the motorette before epoxy impregnation.

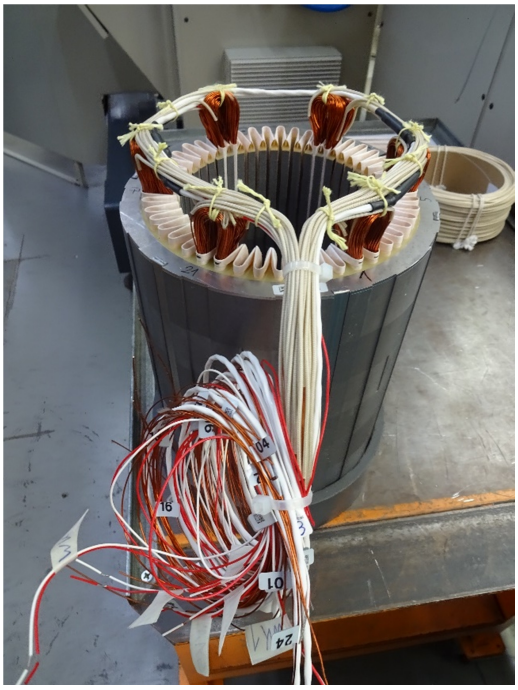

Figure 3.12: Motorette before epoxy Impregnation

3.13.1 DC Test

3.13.1.1 DC Polarization Test

This test is performed to measure the Insulation resistance and leakage current from the excited coils. The measurement can be destructive as well as non-destructive with respect to the amplitude of excitation voltages. There are four parameters of interest from this test

1. Insulation Resistance (IR)
2. Polarization Index (PI)
3. Dielectric Absorption Ratio (DAR)
4. Leakage Current (in nano Amperes)

The tests are performed between the 2 winding terminals as well as between the winding terminal and core of the machine (ground point). The test of insulation

material at an initial state is done before accelerated aging tests are done on the specimen. This test should also be done at regular intervals to observe the trend in changing parameters as the aging test is being carried out. For example, the test could be done at every 100 cycles (more accurate no. after some experience). The main parameter of interest here is the IR and trends with varying IR will be studied as the motorette specimen ages. The IR will be measured for both winding to winding and winding to ground scenarios. A high DC voltage is applied to the coils and the leakage current is measured using the sensitive ammeter inside the Meg-ohmmeter and the IR is calculated using Ohm's law for that time instant. The magnitude of the DC voltage can be chosen according to the ratings of the windings in the machine [18].

For this test a Megger instrument was used to measure the Insulation Resistance and leakage current. The Polarization Index and Dielectric Absorption Ratio can be calculated as follows

$$PI = \frac{IR_{10min}}{IR_{1min}} \tag{3.13}$$

$$DAR = \frac{IR_{1min}}{IR_{30sec}} \tag{3.14}$$

Fig 3.13 and Fig 3.14 shows the connection diagram for High voltage Insulation resistance test for winding to winding and winding to ground scenarios respectively.

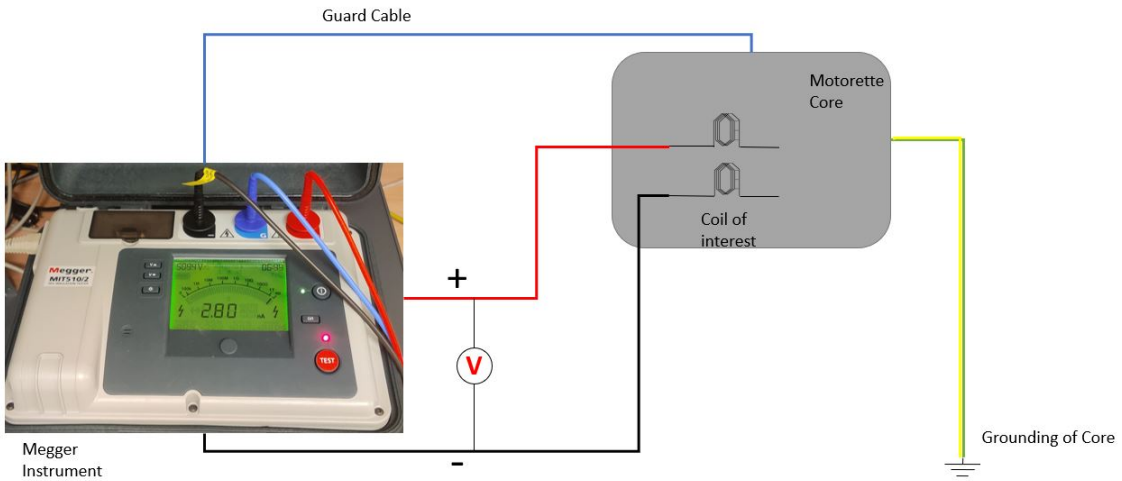

Figure 3.13: Winding to Winding Insulation Resistance Measurement

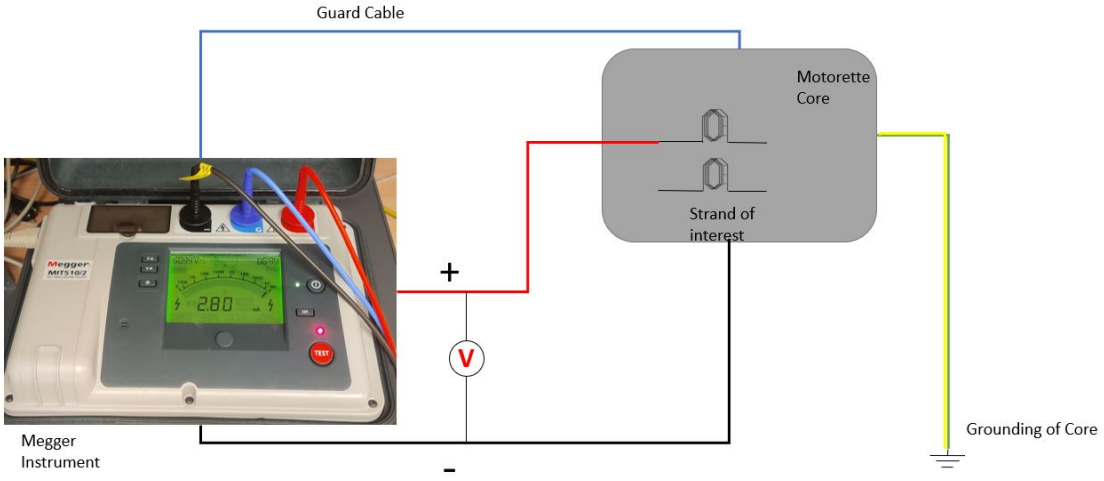

Figure 3.14: Winding to Ground Insulation Resistance Measurement

Table 4.1 below shows the guidelines for the Voltage to be applied depending on the ratings of the winding in the motor.

Table 3.9: Guidelines for DC Voltages to be applied during IR test

Winding Rated Voltage(V)	**Insulation resistance test direct voltage(V)**
<100	500
1000 - 2500	500 - 1000
2501 - 5000	1000 - 2500
5001 - 12000	2500 - 5000
>12000	5000 - 10000

Table 3.10: Winding condition in stator on basis of PI and DAR value

Insulation resistance condition	**DAR**	**PI**
Dangerous	0-1.0	0-1
Poor	1.0-1.3	1-2
Good	1.3-1.6	2-4
Excellent	1.6 and above	4 and above

3.13.2 AC Tests

3.13.2.1 Insulation Capacitance Test

The capacitance test is done on the windings to indicate problems of thermal deterioration or to investigate the presence of moisture in the insulation bulk. This test is most useful on smaller random wound or form wound motors which are water cooled to detect the presence of leaks from the cooling jacket onto the stator

windings. These tests are also done during the end of line (i.e. when the machine is manufactured completely) and also before VPI before epoxy/resin impregnation.

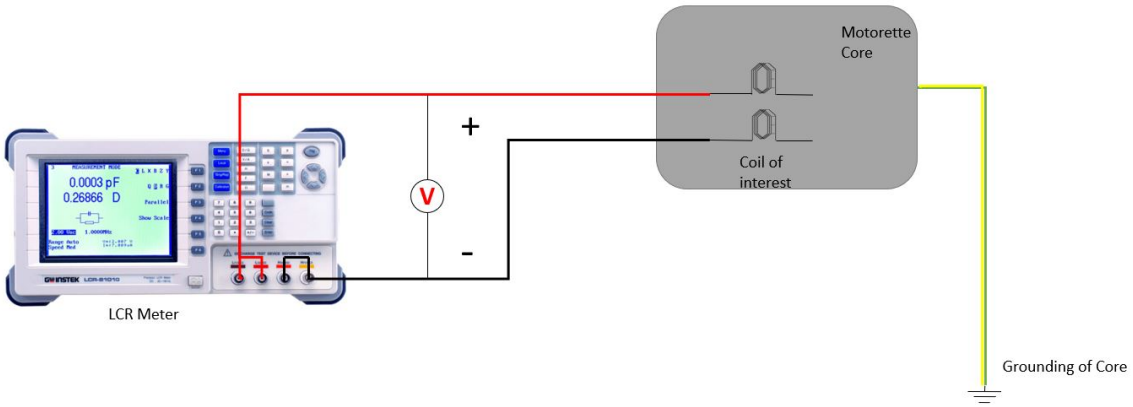

Figure 3.15: Insulation Capacitance measurement

3.13.2.2 Dissipation Factor

The dissipation factor test gives information about the dielectric losses within the insulation. Factors like thermal deterioration and moisture in the insulation will result in an increase in these dielectric losses. The trends in dielectric losses over the age of the machine is the indication of certain types of insulation faults and degradation. The dissipation factor test is also performed by motor manufacturers to check if the resin / epoxy in cured completely after VPI.

4

Results

4.1 Thermal Cycling

The objective of the test rig setup is to perform thermal cycling of the test object with the required minimum and maximum temperatures. As can be seen in Figures 4.1, 4.2, 4.3, 4.4, the test object was cycled from 150°C to 200°C repeatedly. The resistivity of Copper in the strands of the test objects increases with temperature. Thus, the resistance of the strands increases from 4.2Ω at room temperature to 6.65Ω at 200°C (of all 6 strands combined). Accordingly, the voltage drop across the test object increases from 86.2V at room temperature to 136.3V at 200°C.

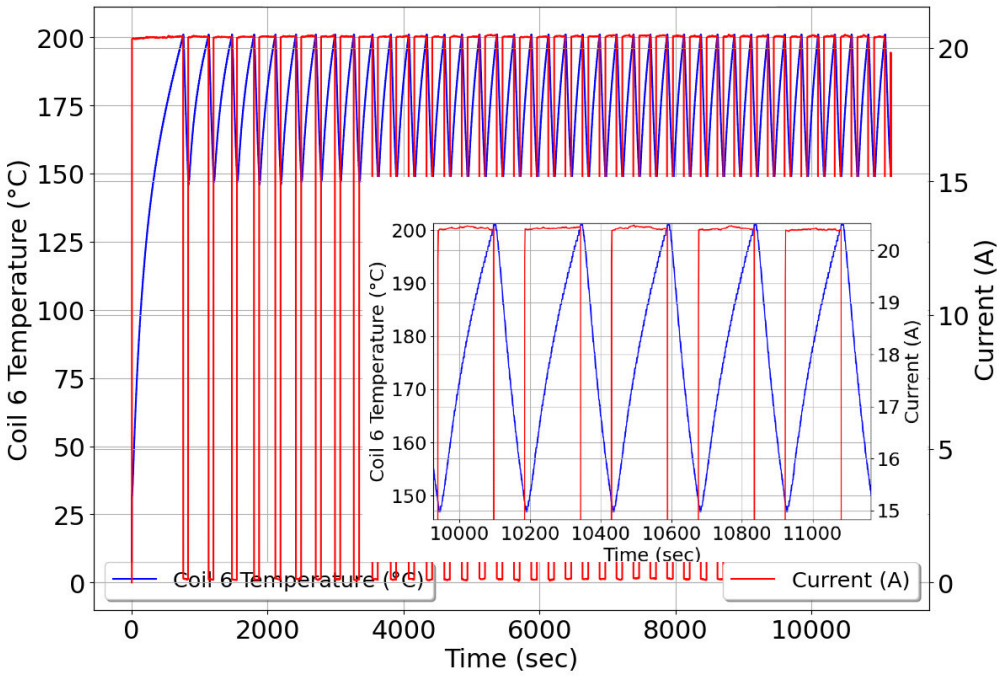

Figure 4.1: Current and temperature of coil 6

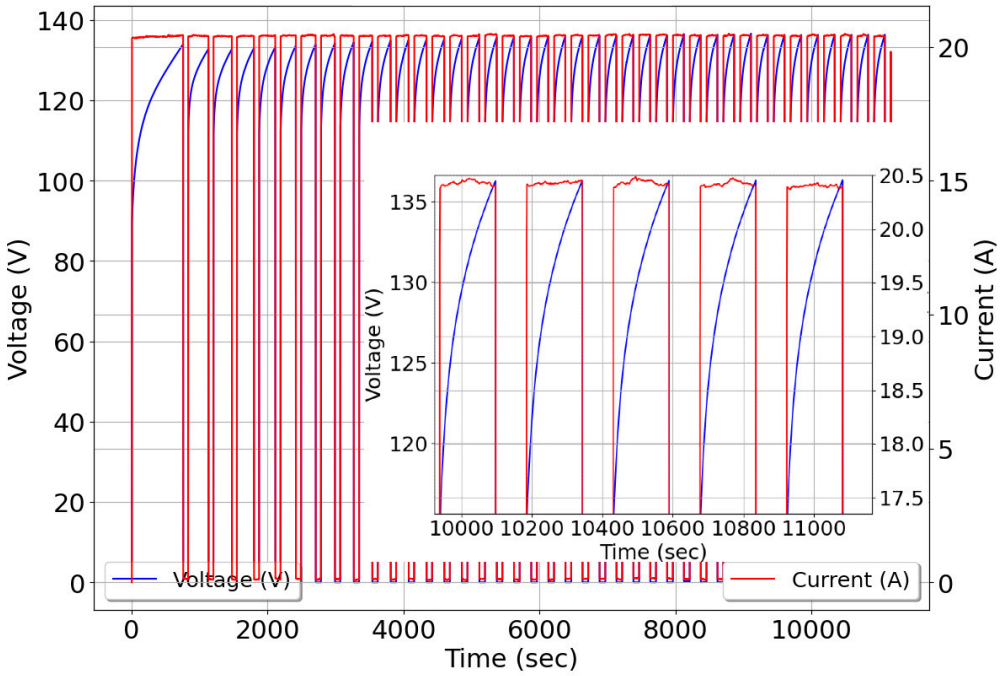

Figure 4.2: Voltage and current through the test object

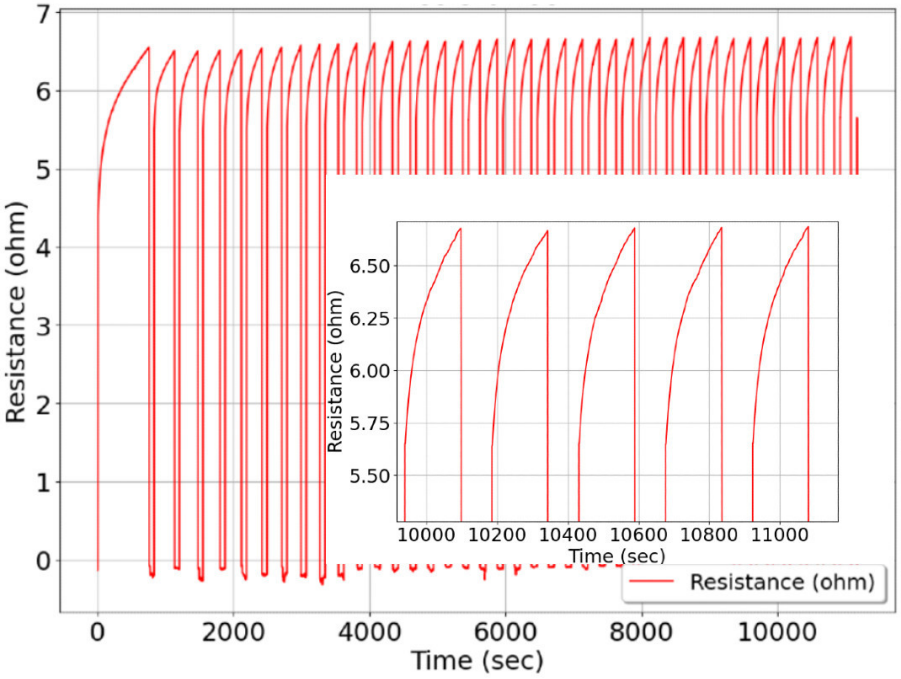

Figure 4.3: Resistance of coil 6

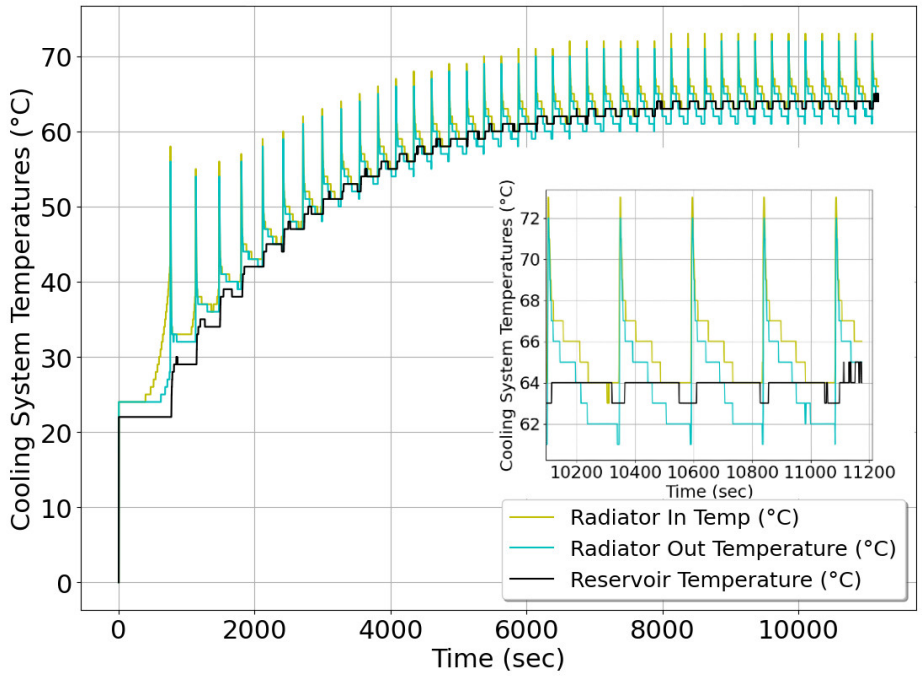

Figure 4.4: Cooling temperatures of test rig

4.2 Insulation Parameters

Thermal cycling on the test object was done to study the variations of insulation parameters. A total of 500 thermal cycles were performed on the test object. The manual measurement of insulation parameters was done at every 100 cycles and initially when the test object was not exposed to thermal stress. The measurement of insulation parameters were done according to Table 4.1

Table 4.1: Measurement voltage levels

Test Type	Voltage Level	Point of measurement	Frequency
DC	1000V	winding to winding	NA
DC	5000V	winding to winding	NA
DC	5000V	winding to ground	NA
AC	1.00V	winding to winding	10kHz

The insulation parameters of interest are listed in Table 4.2 along with the equipment used for their respective measurement.

Table 4.2: Insulation parameters of interest and Equipment used for measurement

Insulation Parameter	Equipment
Insulation Resistance	Megger
Polarization Index	Megger
Dielectric Absorption Ratio	Megger
Insulation Capacitance	LCR Meter
Dissipation Factor	LCR Meter

The coils of interest are Coil 1, Coil 5 and Coil 6 as they have experienced the least, moderate and highest thermal stress as per the temperature log data of the thermal cycles respectively. The measurement of insulation parameters were done when the test object was at room temperature so as to avoid any impact of high coil temperatures on the readings.

4.3 Insulation Resistance Trend

4.3.1 Winding to Winding case

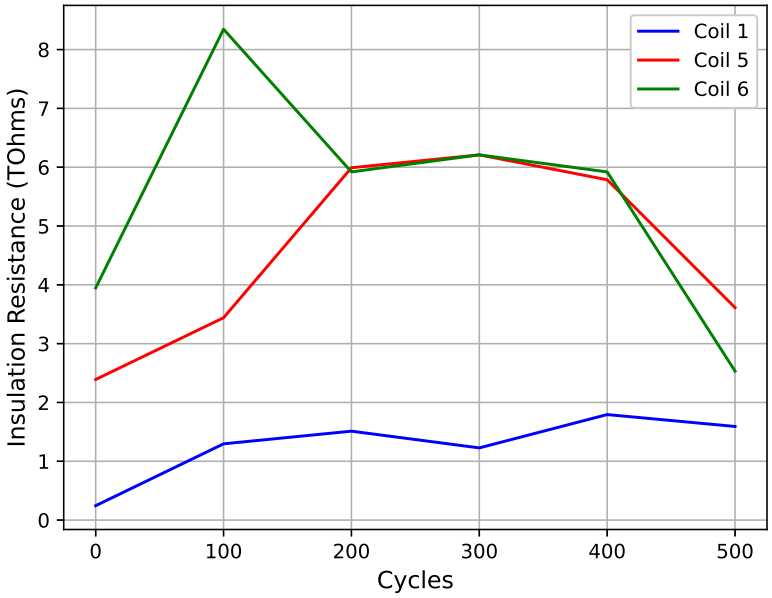

Figure 4.5: Winding to winding insulation resistance trend

The trend from Fig 4.5 shows an increase in insulation resistance in all 3 coils of interest. This increase in insulation resistance is likely due to the absence of moisture presence after the first 100 thermal cycles. The presence of moisture in the insulation could be due to the manufacturing process, direct exposure to moisture during the logistics of the motor and other ambient factors present in the laboratory.

As expected the Insulation resistance drops further as the test object is cycled more due to increased thermal stress. As motors have an approximate lifetime of 10 - 20 years. thermal cycle data of 500 cycles is insufficient to draw conclusions on the variation of insulation resistance change and hence the test object needs to be cycled up to 20,000 cycles which is not within the scope of this master thesis work and should be considered as a future scope.

4.3.2 Winding to Ground case

The trend from Fig 4.6 shows no change in insulation resistance when coil 5 and coil 6 are considered. Coil 1 shows more variation with an increase in beginning due to the presence of moisture and then steep decrease until 400 thermal cycles. As stated earlier, thermal cycle data of 500 cycles is insufficient to draw conclusions on the variation of insulation resistance change and hence the test object needs to be cycled up to 20,000 cycles.

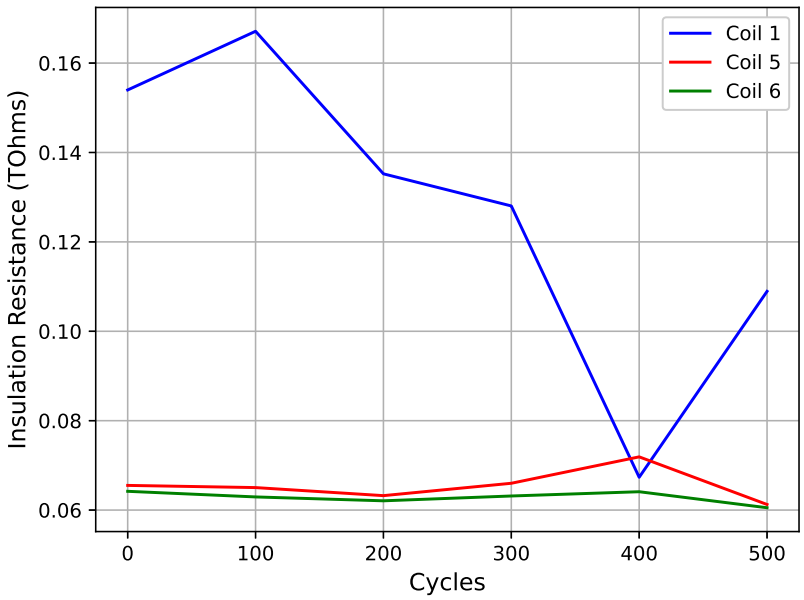

Figure 4.6: Winding to ground insulation resistance trend

4.4 Polarization Index and Dielectric Absorption Ratio Trend

The Polarization Index trend in Figure 4.7 shows the insulation resistance condition after every 100 cycles. As per the typical values of PI from Table 4.1 it is clear that coil 1 has a poor insulation condition right from the start whereas coil 5 and coil 6 show good winding to winding insulation health from the beginning.

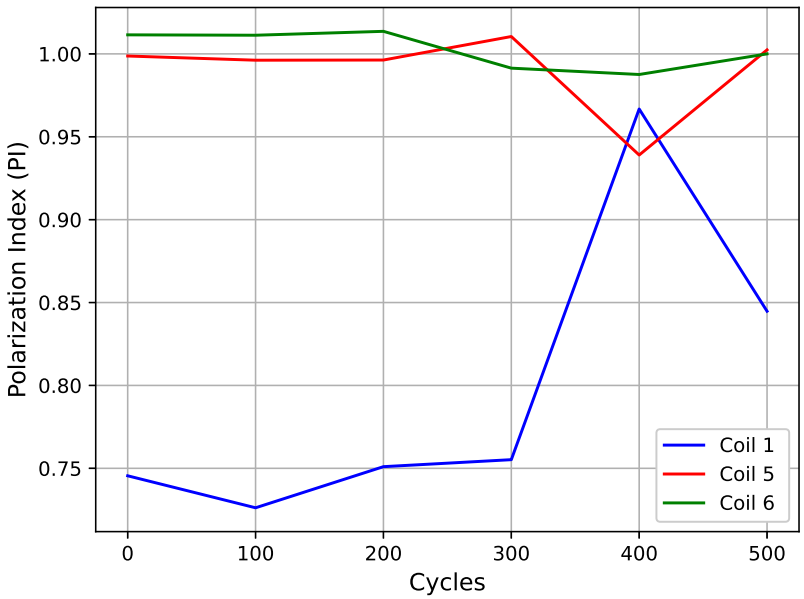

Figure 4.7: Polarization Index trend for winding to winding case

On the contrary when we take a case of winding to ground, we see from Figure 4.8 that all the three coils have a good insulation health as the PI value is greater than 2 after 200 cycles and further thermal cycling is needed to cause degradation to the EIS.

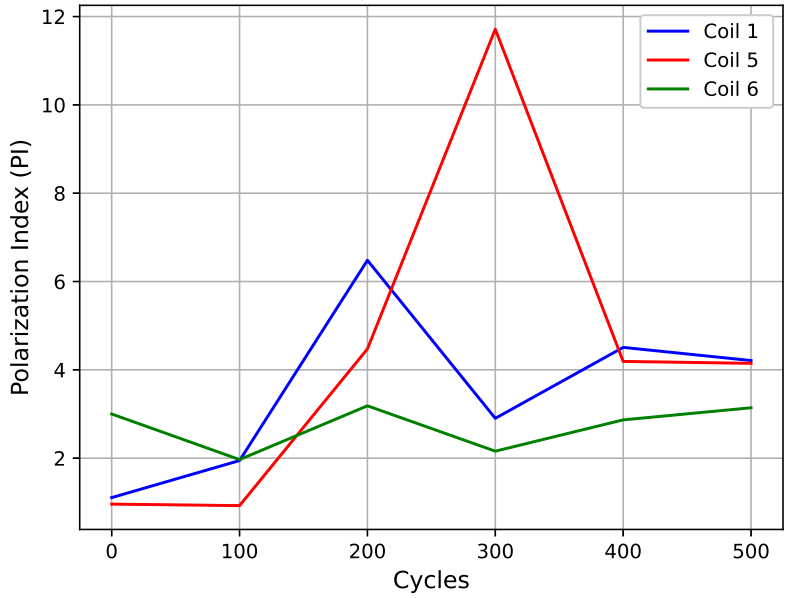

Figure 4.8: Polarization Index trend for winding to ground case

The Dielectric Absorption Ratio trend in Figure 4.9 shows the insulation resistance

condition after every 100 cycles. As per the typical values of DAR from Table 4.1 we can say that the insulation condition between the winding to winding case is of good health.

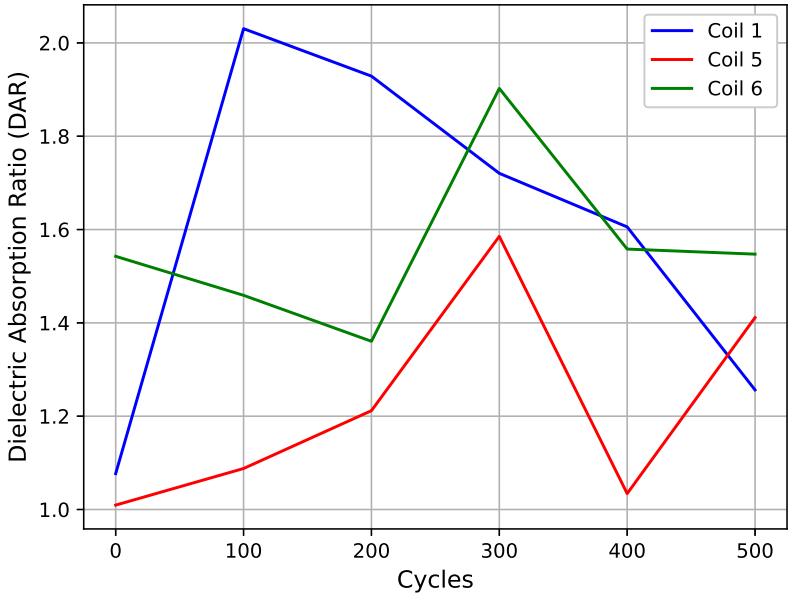

Figure 4.9: Dielectric Absorption Ratio Trend for winding to winding case

On the contrary, from the Figure 4.10 the DAR value for the winding to ground case is between 0 and 1.0 for all the three coils which according to the Table 4.1 means that the insulation condition is of poor health.

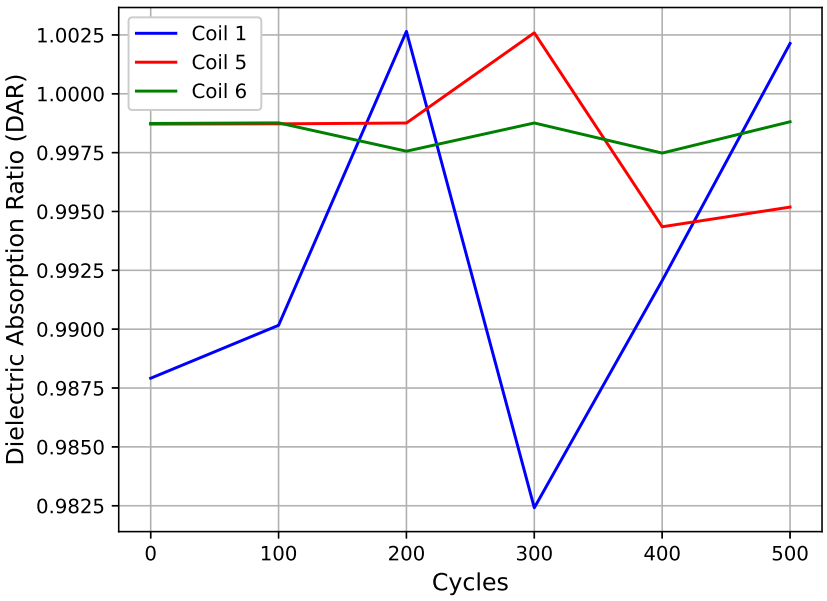

Figure 4.10: Dielectric Absorption Ratio Trend for winding to ground case

4.5 Insulation Capacitance Trend

The trend in insulation capacitance (IC) is shown in Figure 4.11 with respect to the thermal cycles between the windings. The initial dip in the insulation capacitance is due to the presence of moisture in the motorette specimen which causes the insulation capacitance value to be higher than actual and after thermal cycling it comes back to its original value. Coil 5 and coil 6 follow a similar trend as they have been exposed to more stress compared to coil 1 and hence this is also reflected in the insulation capacitance trend.

The trend in dissipation factor (DF) is shown in Figure 4.12 with respect to the thermal cycles between the windings. The dissipation factor trend sees irregularities in the values after every 100 cycles in the case of coil 5 and coil 6. This behaviour cannot be justified with the present data at hand and more thermal cycling on the test object is needed to get a more clear picture of the same.

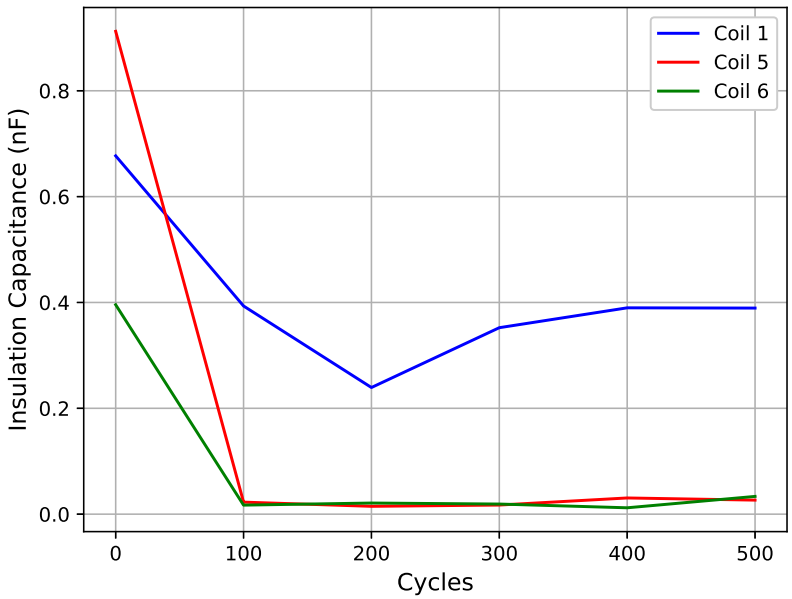

Figure 4.11: Insulation Capacitance Trend

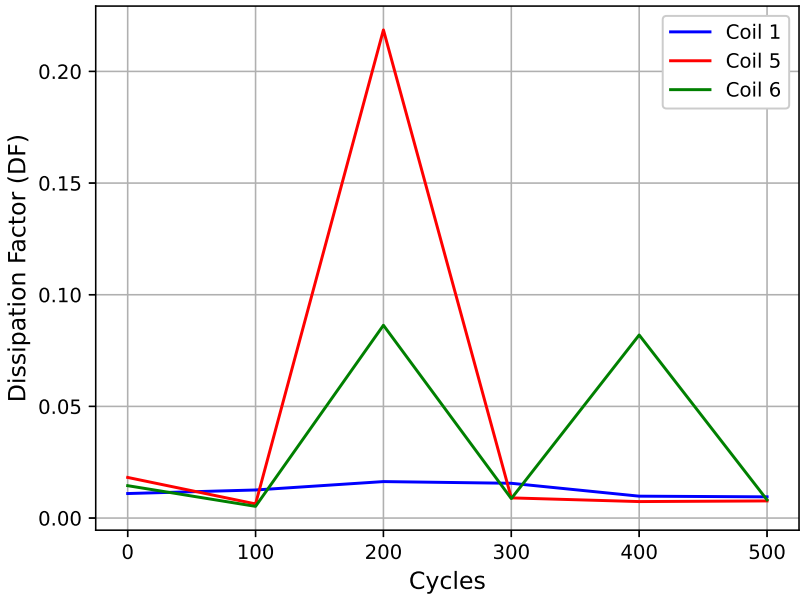

Figure 4.12: Dissipation Factor Trend

4.6 Variation in AC Resistance between strands

The inductance of the strand depends on the position of winding in the slot. Winding positioned deeper into the slot will have higher inductance compared to the ones

positioned near the air gap. The reason for the difference is the component of the magnetic flux which passes transversely to the slots.

The strand current will be distributed depending on the path impedance of the strand. The current in a strand with high inductance will be lower and more phase shifted. Hence when a measurement using the LCR meter is taken it shows that the strand with higher inductance also has higher AC resistance even if the DC resistance of the strands are same. This has also been verified in the study conducted in [19]

This is valid only for Coils 1 -4 in our case. Coils 5 6 have similar AC resistance and Inductance of the strands. The only possible reason behind this is that the 2 strands for coils 5 6 were wound at the same time whereas in case of coil 1-4 strand 1 was wound before strand 2.

4.7 Cooling Efficiency Test

We also wanted to quantify the efficiency of our cooling system, to investigate whether the cooling system performs as expected. Hence, we conducted a test to find how long it takes to cool the test object from 200°C to 100°C. This was done once with the cooling system attached to the test object. Then, we drained the test object of all the water inside the cooling jackets, removed the cooling system and performed the test again.

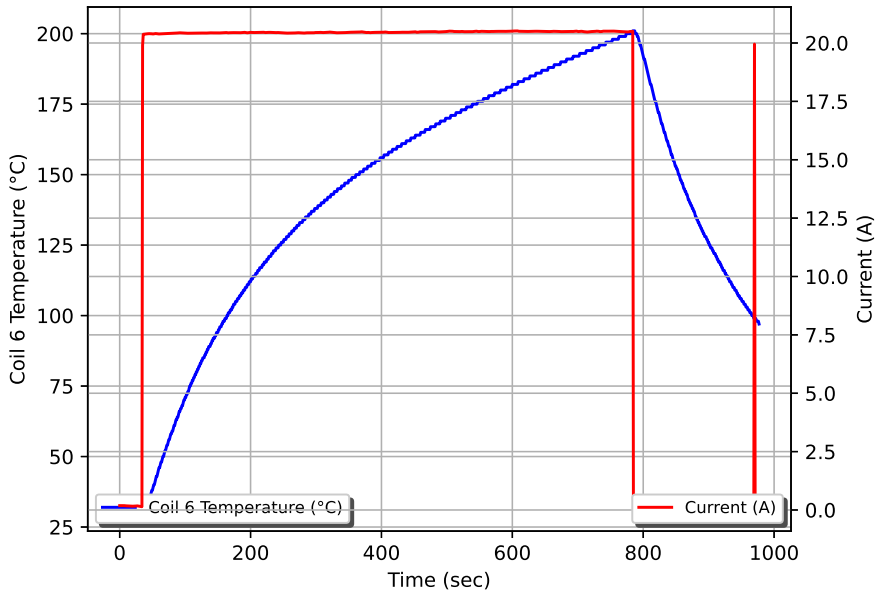

Figure 4.13: Temperatures of Coil 6 with cooling

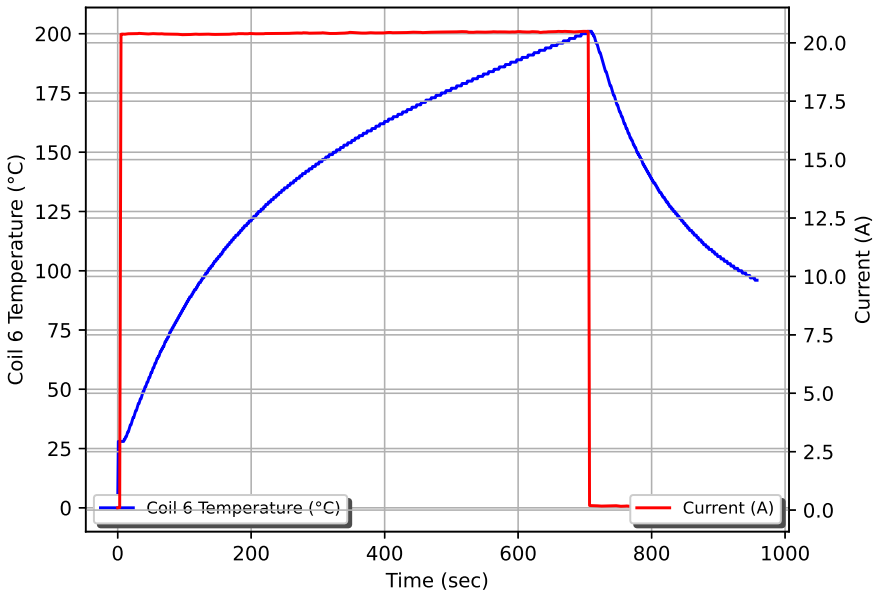

Figure 4.14: Temperatures of Coil 6 without cooling system

Table 4.3: Time taken for the Test Object to Cool

With Cooling (s)	Without Cooling (s)
182	253

The results of the test are given in Figure 4.13, Figure 4.14 and Table 4.3. It can be seen that the cooling system makes a difference in time taken to cool the test object. For this particular test, we see that time taken to cool to 100°C has decreased by 39%.

Furthermore we also compared the heat transfer in both the cases when the motorette is water cooled and when the motorette is cooled using natural convection and radiation. A stationary test was performed to record the steady state casing temperature in presence of coolant which was observed to be 65° and in absence of coolant it was recorded as 118°. The ambient lab temperature was 25°C. Hence ΔT is 40°. Table 4.4 gives a more detailed analysis for various scenarios with different conditions.

We have considered 3 heat transfer coefficients 5 when there is no air flow, 10 when there is some air flow and 30 when there is a lot of air flow. This can be compared to a real life scenario in case of a truck when the truck is at stand still, when a truck is in motion in urban areas and when a truck is on a speedway at maximum speed limit. Also three areas were considered in this case as effective area for heat transfer may vary from setup to setup.

Table 4.4: Heat Transfer without cooling

Change in Temperature ΔT	**Heat Transfer Coefficient α**	**Area (m2)**	**Heat Transfer (W)**
40°	**5**	**0.2**	**40W**
40°	**10**	**0.2**	**80W**
40°	**30**	**0.2**	**240W**
40°	**5**	**0.3**	**60W**
40°	**10**	**0.3**	**120W**
40°	**30**	**0.3**	**360W**
40°	**5**	**0.4**	**80W**
40°	**10**	**0.4**	**160W**
40°	**30**	**0.4**	**480W**

With cooling introduced in the test bench it was possible to dissipate 2.794 kW compared to when heat transfer is approximated in the above cases presented in Table 4.4. This clarifies that there is need for a cooling system to be present in the test bench and components used in the cooling system of the current test bench are borderline adequate for use and there is need to change the radiator core with enhanced air flow rate or substitution of radiator is also possible by a heat ex-changer for improved cooling.

5
Conclusion

5.1 Conclusion

In this thesis, thermal degradation and insulation parameter diagnostics of electric machines were investigated. A test bench for thermal cycling of a test object were set up and 500 thermal cycles were also completed. Insulation parameters of the EIS were measured every 100 cycles. In Chapter 1, some of the previous work on electric machines and EIS were studied and the main objectives of the thesis were laid out. In Chapter 2, degradation of electric insulation and the various stresses that cause the same are presented. Different industry test standards for EIS were investigated and preliminary considerations for the test bench setup were discussed. In Chapter 3, the design of the test rig was presented, including the connection diagram, measurement equipment, data acquisition setup, high voltage and low voltage circuitry. The GUI developed for real time monitoring and implementation automated test logic was discussed. In Chapter 4, results of the thermal cycling tests performed on the test object was presented. This includes plots of the test parameters logged during the tests and the insulation parameters measured at uniform intervals. Although initial variations in the insulation parameters are noticed, comments on degradation of the insulation could not be made as the number of thermal cycles performed on the test object was too low.

5.2 Sustainability Aspects

5.2.1 Ecological Aspects

As the automotive industry transitions to electric and sustainable transportation, it is important to note that these new vehicles are not completely emission free. Although they do not emit tailpipe emissions, they indirectly affect the environment due to the mining and manufacturing of the components in an electric vehicle.
Batteries require rare earth elements, which are often toxic. Electric machines are an important component of electric vehicles, as they replace the internal combustion engine to enable truly zero emissions, at least during usage on roads. Some emissions do occur during their manufacturing, especially while mining for elements in components such as magnets and copper windings. However, we would like to maximize the lifespan of these machines as this would further reduce the overall environmental impact of the automotive industry. Electric machines that have prolonged lifespan reduce the need for more mining operations which are inherently detrimental to the

environment. By investigating the lifespan of insulation and knowing their causes for failure, we can design these machines to last longer.

5.2.2 Economical Aspects

As we move closer to a battery centred ecosystem in the case of next generation automobiles, electric machines will serve as integral parts of the e-powertrains. This will directly and indirectly have an impact on various industries leading to growth, job openings, impact on stock market indexes and development leading to economic growth. The general assembly adopted Agenda for Sustainable Development Goals in 2015 for 2030 is fulfilled by this scenario. Electric mobility is one of the major fostering development offering a new aim for electric machines, which helps in improvement and research towards power output, durability and efficiency.

5.2.3 Social Aspects

Electric powertrains produce lesser noise pollution than their combustion counterparts. This is due to that they have fewer moving parts, which also means that they require lesser maintenance. These powertrains also occupy lesser space, which allows for sleeker frames and more storage space for the user. Electric machines have been in development for longer than combustion engines, and they are widespread in use. However, mining of Neodymium used in permanent magnets [20] and cobalt in batteries [21] often involves child labour and is very toxic to the environment, which should be managed properly.

5.3 Code of Ethics

Many Agencies who commission or fund research or most universities have an ethics committee and publish codes of ethics to scrutinise research proposals to make sure that they wont raise any ethical issues.This section consider IEEE code of ethics to highlight some of the ethical challenges and its measure to avoid them. In focus to follow IEEE code of ethic this section highlight Ethics-1, 5, and 9.

We are performing thermal cycling of a motorette test object, where the same is subjected to currents higher than rated values to accelerate the ageing process. During the test, high voltage and current is run through the test object, which also becomes very hot as almost all the input power is burnt in the test object as heat loss. The operator should be careful and take all safety precautions while performing these tests.

One of the goals of thermal cycling and ageing of a test object is to investigate the lifetime of an electric machine in a traction application. This is important as by predicting the life of a machine, as we can dimension and improve its design according to the application. Also, for the user of the machine, diagnostic information about the health of the machine can help them be aware of required maintenance or chance of failure in the near future.

The challenge involves to seek, accept, offer honest criticism of technical work and to credit properly the contributions of others. This challenges can be handled by offering peer review, provide honest criticism for the their reports with respect and also accept review as well as criticism from them with respect. Acknowledging all the technical document referred for literature survey purpose, also considering everyone's input and idea to the project success.

5.4 Future Work

This thesis work comprises of test bench design and initial thermal cycling on the test object. Due to lack of time it was not possible to finish the entire degradation study and hence following is proposed as future work

1. A minimum of 15000 thermal cycles are suggested to observe significant trends in the insulation parameters and to reach a conclusion about the lifetime of EIS. vehicle.
2. Measurement of Partial Discharge Inception Voltage(PDIV) is recommended after 10000 cycles to detect the presence of air gaps or voids within the insulation.
3. A postmortem analysis on a material level is suggested to study the degradation in mechanical and other surrounding components. This will give the designers a better idea of the manufacturing process and a comparison between the FEM simulation results of stresses that can be done with the actual test object.
4. Also an analogy between thermal cycles to drive cycles is needed to understand how much does 1 thermal cycle is equivalent in terms of driven distance in case of an electric vehicle.
5. Thermal cycling on one test object might not be enough to certify the ageing criteria and hence this should be done on 10 such objects and then later by means of statistical evaluation such as variation in life (in hours), statistical distributions (like Gaussian and log-normal distribution) we can generate ageing models based on regression analysis.
6. Certain destructive tests can also be performed at End of life (EOL) to study other parameters in the construction of the machine and EIS.
7. Improvisation on the current cooling system setup as suggested in the results section is also necessary to perform thousands of thermal cycles.

Bibliography

[1] W. Xu, J. Zhu, Y. Guo, S. Wang, Y. Wang, and Z. Shi, "Survey on electrical machines in electrical vehicles," in *2009 International Conference on Applied Superconductivity and Electromagnetic Devices*, 2009, pp. 167–170.

[2] Z. Q. Zhu and C. C. Chan, "Electrical machine topologies and technologies for electric, hybrid, and fuel cell vehicles," in *2008 IEEE Vehicle Power and Propulsion Conference*, 2008, pp. 1–6.

[3] T. Hakamada, "Analysis of weibull distribution for electrical breakdown voltage o stator windings," *IEEE Transactions on Electrical Insulation*, vol. EI-19, no. 2, pp. 114–118, 1984.

[4] P. Cygan and J. Laghari, "Models for insulation aging under electrical and thermal multistress," *IEEE Transactions on Electrical Insulation*, vol. 25, no. 5, pp. 923–934, 1990.

[5] P. Tavner and J. Hasson, "Predicting the design life of high integrity rotating electrical machines," in *IEMDC 1999*, 1999.

[6] Megger. (2021) A stich in time - the complete guide to electrical insulation testing. [Online]. Available: https://us.megger.com/promotion/vf/social-media/stitch-in-time-instant-download

[7] G. Pellegrino, A. Vagati, B. Boazzo, and P. Guglielmi, "Comparison of induction and pm synchronous motor drives for ev application including design examples," *IEEE Transactions on Industry Applications*, vol. 48, no. 6, pp. 2322–2332, 2012.

[8] G. C. Stone, E. A. Boulter, I. Culbert, and H. Dhirani, *Electrical insulation for rotating machines: design, evaluation, aging, testing, and repair*. John Wiley & Sons, 2004, vol. 21.

[9] (2021) Insulator (electricity). [Online]. Available: https://simple.wikipedia.org/wiki/Insulator_(electricity)

[10] S. Roberts. (2021) What are electrical insulators? [Online]. Available: https://www.wise-geek.com/what-are-electrical-insulators

[11] A. Upadhyay, M. Alaküla, and F. J. Márquez-Fernández, "Characterization of onboard condition monitoring techniques for stator insulation systems in electric vehicles-a review," in *IECON 2019-45th Annual Conference of the IEEE Industrial Electronics Society*, vol. 1. IEEE, 2019, pp. 3179–3186.

[12] J. Härsjö, *Modeling and analysis of PMSM with turn-to-turn fault*. Chalmers Tekniska Hogskola (Sweden), 2016.

[13] A. Reinap and A. Upadhyay, "Specification of a specimen for accelerated thermal aging tests," in *2019 IEEE 12th International Symposium on Diagnostics*

for Electrical Machines, Power Electronics and Drives (SDEMPED). IEEE, 2019, pp. 49–55.

[14] IEC-60085, "Electrical insulation - thermal classification," 2004-6.

[15] IEC-60216-1, "Electrical insulating materials–thermal endurance properties. part 1: ageing procedures and evaluation of test results," 2013.

[16] IEC-61857-21, "Electrical insulation systems - procedures for thermal evaluation - part 21: Specific requirements for general-purpose models - wire-wound applications," 2009.

[17] IEC-60611, "Guide for the preparation of test procedures for evaluating the thermal endurance of electrical insulation systems," 1978.

[18] Z. Huang, "Modeling and testing of insulation degradation due to dynamic thermal loading of electrical machines," *Ph. D. thesis*, 2017.

[19] H. Hämäläinen, J. Pyrhönen, J. Nerg, and J. Talvitie, "Ac resistance factor of litz-wire windings used in low-voltage high-power generators," *IEEE Transactions on Industrial Electronics*, vol. 61, no. 2, pp. 693–700, 2013.

[20] Y. Enviroment. (2019) China wrestles with the toxic aftermath of rare earth mining. [Online]. Available: https://e360.yale.edu/features/china-wrestles-with-the-toxic-aftermath-of-rare-earth-mining

[21] T. Guardian. (2016) Children as young as seven mining cobalt used in smartphones, says amnesty. [Online]. Available: https://www.theguardian.com/global-development/2016/jan/19/children-as-young-as-seven-mining-cobalt-for-use-in-smartphones-says-amnesty

Appendix 1

An overview of the classes written in the code are given below:

my_can class This class is used to setup all the variables and methods that deal with the CAN bus. This includes reading from the DBC files, receiving and sending messages and calling the data logging functions.

my_tk class The my_tk class sets up the main root window for the GUI and configures some parameters for the same. Other classes create frame objects, which are spaces inside the root window with different functionality.

tlb_frame class This class sets up a frame for the channel selector toolbar below each plot.

plt_frame class The plt_frame class sets up the frame for displaying plots inside the root window. Multiple objects of this created to display plots for each CSM module.

bt_switch_frame class This frame class is used to setup the buttons for manual control of the test bench.

e_frame class This frame class is used for setting up user entry fields for the test parameters.

bt_test_frame class This frame class is used for displaying start and stop buttons for the automated test functionality.

postpross_frame class The postpross_frame_class contains buttons for showing and hiding postprocessed data while the bench is running.

lb_frame class This frame class sets up labels for displaying test parameters given as input by the user.

gen_data class This is a generator class that sends CAN bus data to the plt_frame class objects in a memory efficient manner.

my_log class The my_log class object logs data in a CSV file.

main function The main function declares objects of the above classes, assigns grid positions for frame and runs the Tkinter mainloop. It also runs the recv_msg function in a parallel thread to the Tkinter mainloop to get data from the CAN bus. When the test is stopped and the GUI is closed, the data is logged before the program ends.

Appendix 2

A list of equipment used in he test bench setup along with their inventory number is given below.

Table .1: List of Equipment used in test bench

Sr No.	Equipment	Inventory No.
1	Megger 510/2	2010-inv.nr 600
2	Delta Elektronika HV power Supply	2010-inv.nr 148
3	Tektronix A6303 Current Probe	2010-inv.nr 268
4	Low Voltage supply 1	2010-inv.nr 744
5	Low Voltage supply 2	2010-inv.nr 98
6	Fluke Multi meter	2010-inv.nr 704
7	Fluke Multi meter	2010-inv.nr 537
8	GWinstek LCR Meter	2010-inv.nr 1108
8	LeCroy Oscilloscope	2010-inv.nr 964
10	Luca 63A - 16A Switchboard	2010-inv.nr 611

DEPARTMENT OF SOME SUBJECT OR TECHNOLOGY
CHALMERS UNIVERSITY OF TECHNOLOGY
Gothenburg, Sweden
www.chalmers.se

CHALMERS
UNIVERSITY OF TECHNOLOGY